

A semi-analytical model for polymers subjected to high strain rates

Authors:

A. Haufe, DYNAmore GmbH
P.A. Du Bois, Consulting Engineer
S. Kolling & M. Feucht, DaimlerChrysler AG

Correspondence:

Dr. André Haufe
Dynamore GmbH
Industriestr. 2, D-70565 Stuttgart, Germany
Tel.: +49 -711-45 96 00 17
Fax: +49 -711-45 96 00 29
Email: andre.haufe@dynamore.de

Keywords:

Thermoplastics, Explicit Finite Element Method, Crash Simulation,
Material Modelling, Visco-Plasticity, Elastic Damage

Abstract:

Reliable prediction of the behaviour of structures made from polymers is a topic under considerable investigation in engineering practice. Especially, if the structure is subjected to dynamic loading, constitutive models considering the mechanical behaviour properly are still not available in commercial finite element codes.

First, we give an overview of material laws for thermoplastics and show how the behaviour can be characterized and approximated by using visco-elasticity and metal plasticity, respectively. Experimental work is presented to point out important phenomena like necking, strain rate dependency, unloading behaviour and damage. A constitutive model including the experimental findings is derived. In particular, different yield surfaces in compression and tension and strain rate dependent failure, the latter with damage induced erosion, need to be taken into account. With the present formulation, standard verification tests can be simulated successfully. Also, an elastic damage model is used to approximate the unloading behaviour of thermoplastics adequately.

1 Introduction

The numerical simulation of structural parts made from polymers is becoming increasingly important in the context of pedestrian protection, e.g. head and leg impact, see [5], [9] –[11]. Although highly sophisticated material laws are available in commercial finite element programs, there are still open questions, especially for crashworthiness analysis. In this paper, we restrict our attention to the explicit solver of LS-DYNA [1], [2]. However, the results are transferable to other solvers. We give an overview on classical models for polymers which are used for crash simulations nowadays. From a practical point of view, the commonly used model is material #24 (MAT_PIECEWISE_LINEAR_PLASTICITY). However, since thermoplastics are not incompressible during plastic flow, material laws based on *von Mises* plasticity are not suitable. Therefore, we suggest a new material model which has been implemented into LS-DYNA as a user defined material.

Based on experimental work, important phenomena like necking, strain rate dependency, unloading behaviour and damage is presented. Subsequently, a constitutive model including the experimental findings is derived. In particular, different yield loci in compression and tension and strain rate dependent failure, the latter with damage induced erosion, are noticeable properties of a suitable constitutive model that need to be regarded. Taking a three point bending test as an example, we demonstrate the applicability of a *Drucker-Prager* model that takes the compressibility and the different behaviour of the material under tensile and compressive stress into account. A simple elastic damage model is used to approximate the unloading behaviour of thermoplastics herein.

Furthermore, a new constitutive model, termed as *SAMP-0 (Semi-Analytical Model for Polymers with C^0 -differentiable yield surface)*, is derived that shows promising results in standard verification test. Here a pressure dependent multi-surface yield locus is defined. The plastic potential based on the classical *Drucker-Prager* cone may be adjusted to lead to associated and non-associated flow in compression. The well known *von Mises* yield surface, although not applicable for polymers as stated before, is included as special case. Strain rate dependency for the yield surface as well as for the failure onset is another key

property. Furthermore a simple but effective damage formulation that allows smooth fading of elements, that are supposed to fail, is included.

2 Motivation

Under high velocity impact loading, thermoplastic components undergo large plastic deformations and will most likely fail. Consequently, the unloading behaviour is irrelevant and thermoplastics can be modelled with a pretty good approximation as pseudo-metallic elastic-plastic bodies. This is, however, not always the case. An important application in crash simulation for a more accurate modelling of thermoplastics is the behaviour of a bumper fascia during leg impact in pedestrian protection. Here, it is essential to compute the internal energy of the bumper fascia to determine the correct bending angle of the leg as a measure of loading due to the impact. In this loading case the bumper fascia will typically undergo only small straining and the deflection will be largely elastic. The unloading phase is of fundamental importance for the determination of the bending angle in the leg-form.

The visco-elastic response of the thermoplastic under the yield surface must, consequently, be modelled and this is not the case in traditional elastic-plastic material laws which consider the material response to be linear elastic until yield. In Figure 1, stress-strain curves are depicted for a typical bumper fascia material: A thermoplastic elastomeric olefin resin. The strain rate behaviour is similar to what is known for steels. However, not only an increasing plastic behaviour is detectable if we increase the strain rate; an increasing modulus of elasticity can be measured too. Moreover, a distinct nonlinear elastic part can be observed but cannot be modelled by a purely linear elastic-plastic law as present in this paper.

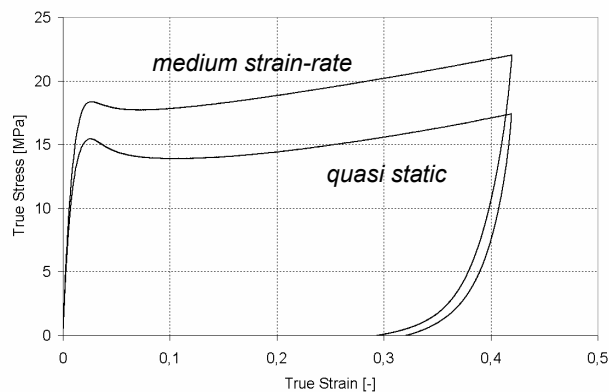


Figure 1: Stress-Strain curves for PP-EPDM

The true stress-true strain curve in *Figure 1* shows a reversal of curvature indicating a softening phase that is followed by a hardening phase. Thus the deformation of a typical dog-bone shaped specimen shows necking at very low strains corresponding to the initial softening of the material. The subsequent hardening, however, results in a stabilization of the necked area and a redistribution of the plastic strains over the entire specimen. Unlike metals, the primary energy-absorbing potential of the thermoplastic resides at plastic strains beyond the necking value.

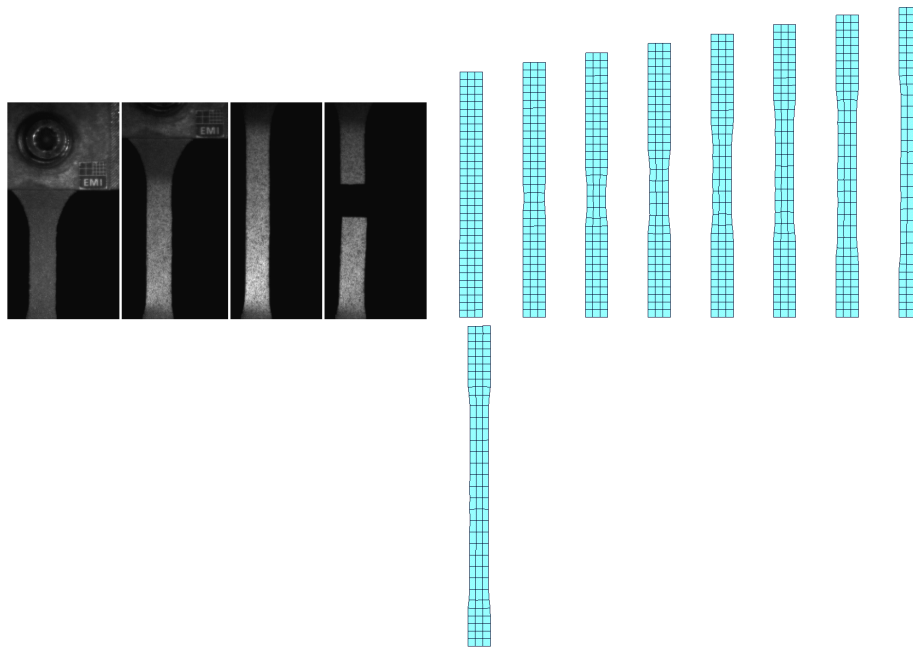


Figure 2: Tensile test and necking simulation of PP-EPDM

This type of physical response can be modelled perfectly using standard elastic-plastic material laws although the plastic deformation of thermoplastics is not isochoric. In Figure 2, the temporal evolution of the necking simulation is shown. A further effect which has to be considered, e.g. for leg impact simulation, is the unloading behaviour of the material. This behaviour can be approximated linearly by a simple damage model decreasing Young's modulus E by $E_{eff} = E(1 - d)$ where $d = \hat{d}(\bar{\epsilon}_{pl})$ is a damage parameter which increases while accumulating the equivalent plastic strains. Usually, this damage parameter can be tabulated directly as a function of the plastic strains.

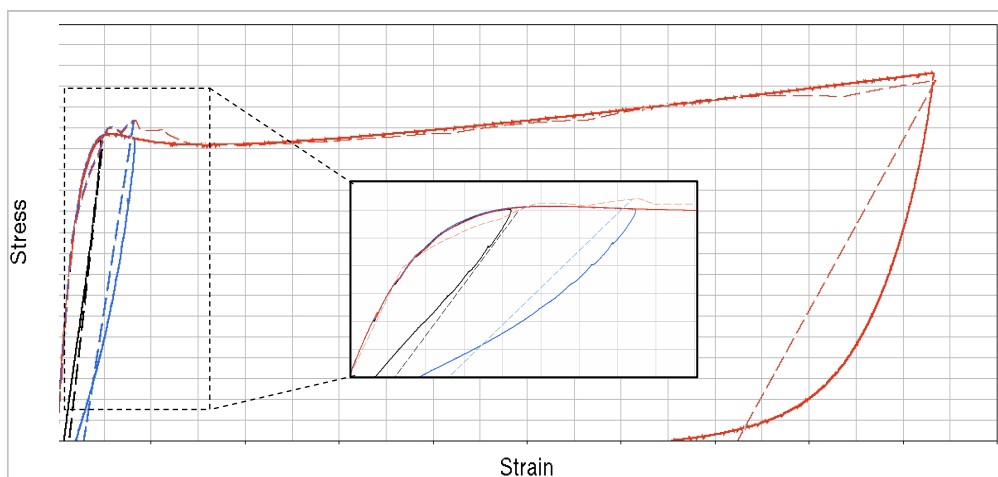


Figure 3: Approximation of the unloading behaviour by damage formulation

It is important to know that the damage parameter also influences the stresses. Therefore, the stress-strain curve has to be modified in such that the updated stresses correspond to the experimental findings:

$$\sigma_y \mapsto \frac{\sigma_y}{(1-d)} \quad (1)$$

The simulation results of a simple tensile test in comparison with experimental results are depicted in Figure 3. As can be seen, the reduction of the elastic parameters for increasing plastic strains considers the unloading behaviour approximately. Finally, the experimental stress-strain curve is recovered.

In the following, we discuss the different behaviour of thermoplastics in compression and tension; see [6] for an overview of various polymers. We investigate the effects of the classical *Drucker-Prager* model (see [7], [8]), which is usually implemented in commercial solvers.

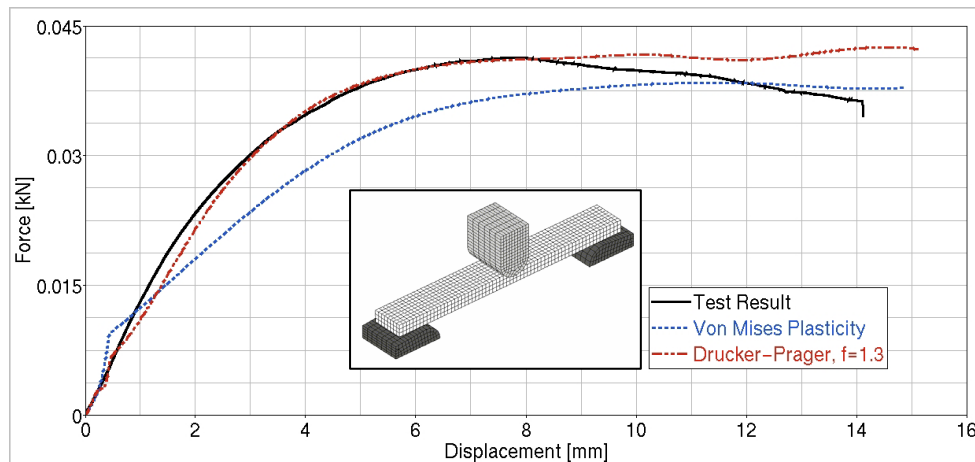


Figure 4: Three-point-bending test

In Figure 4, the reaction force versus the displacement of a quasi-static three point bending test is shown. Because of the higher yield stress under compression, it is not possible to simulate the bending test by using *von Mises* plasticity based on the tensile test data. If a standard *Drucker-Prager* model is used, where the yield stress taken from the experiment under compression is 1.3 times the yield stress under tension [6], the bending test can be simulated with good agreement.

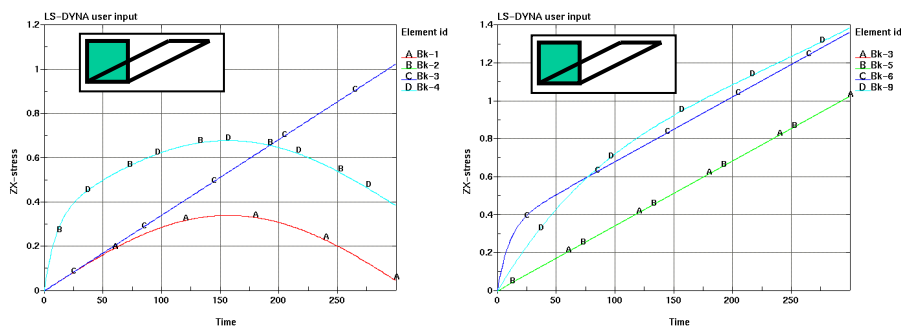
In conclusion it can be said that all the effects associated with thermoplastics can be approximately considered in simple material models: Necking by an elastic-plastic law, unloading behaviour by a damage model, different behaviour under compression and tension e.g. by a standard *Drucker-Prager* model. A material model which covers all these effects is proposed in what follows.

3 Material Formulations

In an industrial oriented environment, only limited time is available to produce reliable and sound simulation results. The most efficient material laws from a user point of view are undoubtedly based on tabulated stress-strain curves obtained directly from physical testing. That way, although some smoothing of the raw test data may be required for reasons of numerical stability, time-consuming fitting operations needed for analytical formulations can be entirely avoided. It should be emphasized however, that predictable analysis is necessarily based on experimental material testing. In what follows, we briefly review the main classes of material formulations as they are implemented in the LS-DYNA package.

3.1 Visco-elasticity

Visco-elastic material laws in LS-DYNA are based on hypo-elasticity. In such a hypo-elastic formulation, the objective stress rate is derived directly from the strain rate or the rate of deformation tensor. In the particular case of LS-DYNA, stress rates according to *Jaumann* are chosen. It is well known, that the use of the *Jaumann* rate leads to an oscillatory response under large shear deformations. The difference between hyper- and hypo-elasticity in the case of simple shear is illustrated in Figure 1a, curve A (hypo-elastic) and C (hyper-elastic, *Blatz-Ko*). It can be seen clearly from the picture that the differences are negligible for small shear strains. It should be emphasized that problems with hypo-elastic material laws only occur for large deformations and not for large rotations. Therefore, hypo-elastic formulations are adequate for the description of large rotation/small deformation problems.



a) Material 1(A), 6(B), 7(C) and 76(D)

b) Material 7 (A) and 77 (B,C,D)

Figure 5: Simple shear behaviour for hypo- and hyper-elastic materials

Hypo-elasticity is easily generalized to include time-dependency of the stresses. However, in this case the reversibility of the material law is lost. This allows considering phenomena such as hysteresis, rate dependency, stress relaxation and creep. In linear hereditary material laws or *Boltzmann* laws, deviatoric stresses s and hydrostatic stresses p are computed by a convolution integral of the strain rate and the relaxation function:

$$s = \int_0^t 2g(t-\tau) \dot{\epsilon}_d(\tau) d\tau, \quad p = \int_0^t k(t-\tau) \dot{\epsilon}_v(\tau) d\tau \quad (2)$$

In this equation $\dot{\epsilon}_d$ represents the deviatoric and $\dot{\epsilon}_v$ represents the volumetric strain rate; the convolution integrals are evaluated from zero until the current time t . The relaxation functions g and k are nothing else than time-dependent moduli, i.e. if the function is constant in time, hypo-elasticity is recovered through $g=G$ and $k=K$. The resulting stresses are linear in the strain rate which is typical for polymers at small strain. Note that linear visco-elasticity is often based on a *Prony* (exponential) series where up to six exponential terms are used in the relaxation function.

In Figure 5, some simple shear test simulation results are presented. The test was simulated using a single solid element as illustrated by the insert in the upper left hand corner. The solid element refers to different hyper- and visco-elastic material models available in the LS-DYNA code: hypo-elastic (material no. 1), visco-elastic (material no. 6), general visco-elastic (material no. 76), Blatz-Ko (material no. 7) and Ogden (material no. 77), see [1] for details. A linear response is obtained for the quasi-static case where hyper-elastic material laws

are used, compare curves A and B in Figure 5b and curve C in Figure 5a. Hypo-elastic material laws show the well known *Jaumann* rate type of response (curve A in Figure 5a). In the dynamic case, LS-DYNA uses a *Jaumann* formulation to evaluate the viscous stress terms as can be seen in curves B and D in Figure 5a. Depending on the used relaxation times, the *Jaumann*-type effects will be more or less pronounced, see curves C and D in Figure 5b.

| Law | Keyword |
|-----|---------------------------------|
| 6 | MAT_VISCOELASTIC |
| 60 | MAT_ELASTIC_WITH_VISCOSITY |
| 61 | MAT_KELVIN-MAXWELL_VISCOELASTIC |
| 62 | MAT_VISCOUS_FOAM |
| 76 | MAT_GENERAL_VISCOELASTIC |

Table 1: Overview of visco-elastic materials in LS-DYNA

A selection of visco-elastic laws which are available in LS-DYNA are listed in Table 1. Visco-elastic material models are often suitable to describe the strain rate dependent behaviour of thermoplastics for small strains (strains below 5%). An example, where a visco-elastic law to simulate a polymer material is used, is given in Figure 6. However, it should be emphasized that a lot of work has to be performed for parameter identification.

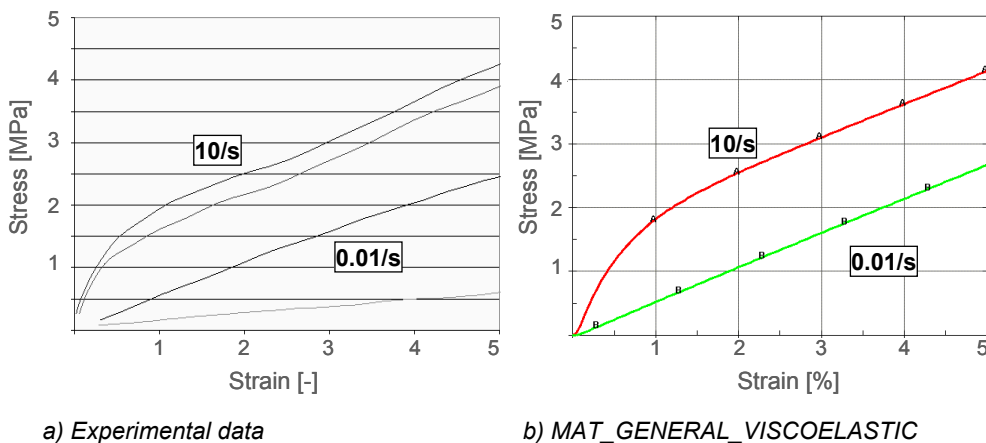


Figure 6: Modelling of a polymer by linear visco-elasticity

3.2 Plasticity

Historically elastic-plastic material laws have been developed for the description of metallic materials based on crystal plasticity. The most commonly used example of this type implemented in LS-DYNA is MAT_PIECEWISE_LINEAR_PLASTICITY (material no. 24). The same approach can be applied to some degree to the simulation of thermoplastics. However, it should be noted that a very important differences exists between metals and thermoplastics. In particular, plastics have no constant modulus of elasticity and the different yield criterions under tension and compression preclude the use of a *von Mises* type of yield surface. Furthermore, the hardening of thermoplastics is anisotropic and the plastic deformation is not volume preserving. This lack of plastic incompressibility requires a flow rule allowing for permanent volumetric deformation. None of these effects can be considered in a classical *von Mises* elastic-plastic material law. For an overview, some constitutive models considering plasticity - limited to materials with isotropic behaviour - are listed in Table 2.

| Law | Keyword | Hardening | Rate effect |
|-----|--|------------|---------------|
| 3 | MAT_PLATIC_KINEMATIC | Linear | CS |
| 12 | MAT_ISOTROPIC_ELASTIC_PLASTIC | Linear | CS |
| 15 | MAT_JOHNSON_COOK | Power law | JC |
| 18 | MAT_POWER_LAW_PLASTICITY | Power law | CS |
| 19 | MAT_STRAIN_RATE_DEPENDENT_PLASTICITY | Linear | load curves |
| 24 | MAT_PIECEWISE_LINEAR_PLASTICITY | Load curve | CS, tabulated |
| 81 | MAT_PLASTICITY_WITH_DAMAGE | Load curve | CS, tabulated |
| 89 | MAT_PLASTICITY_POLYMER | Load curve | CS, tabulated |
| 98 | MAT_SIMPLIFIED_JOHNSON_COOK | Power law | JC |
| 105 | MAT_DAMAGE_2 (Visco-plastic) | Power law | Perzyna |
| 112 | MAT_FINITE_ELASTIC_STRAIN_PLASTICITY | Load curve | CS, tabulated |
| 123 | MAT_MODIFIED_PIECEWISE_LINEAR_PLASTICITY | Load curve | Load curve |

Table 2: Overview of plastic materials in LS-DYNA

3.3 A modified approach with respect to thermoplastics

Originally, all plasticity models listed in Table 2 are developed for metals. They are based on *von Mises* plasticity. However, this type of plasticity has some deficiencies with respect to thermoplastics (although one might think MAT_PLASTICITY_POLYMER could be suitable). The main drawback is the assumption of plastic incompressibility which is clearly not correct for thermoplastics. From this point of view, there is a strong need for a new material model. In our approach, we use a modified *Drucker-Prager* model based on the general ideas of [12]. This model will be termed *SAMP-0* further on.

Within this model additive decomposition of the strain increment $\Delta\boldsymbol{\varepsilon}^{tot} = \Delta\boldsymbol{\varepsilon}^{el} + \Delta\boldsymbol{\varepsilon}^{pl}$ is assumed. This leads to an elastic stress increment according to $\Delta\boldsymbol{\sigma} = \mathbf{C}^{el} : \Delta\boldsymbol{\varepsilon}^{el}$ where the elastic constitutive tensor reads $\mathbf{C}^{el} = 2G\boldsymbol{\delta} \otimes \boldsymbol{\delta} - (K - \frac{2}{3}G)\boldsymbol{\delta} \otimes \boldsymbol{\delta}$. Here G is the shear and K the bulk modulus and $\boldsymbol{\delta}$ represents the Kronecker delta. The plastic strain components are calculated by a classical elastic predictor-plastic corrector scheme which will be discussed in a forthcoming section.

3.3.1 Definition of SAMP-0 yield surface

The yield surface is composed of two *Drucker-Prager*-cones; f_c for the compression and f_t for the tension region, see Figure 7. Here $p = -\frac{1}{3}\sigma_{xx} = -\frac{1}{3}I_1$ represents the hydrostatic axis and $q = \sqrt{\frac{3}{2}\mathbf{s} : \mathbf{s}} = \sqrt{3}J_2 = \sigma_{vm}$ the deviatoric axis. As usual, I_1 represents the first invariant of the stress tensor $\boldsymbol{\sigma}$ and J_2 the second invariant of the stress deviator $\mathbf{s} = \boldsymbol{\sigma} - \frac{1}{3}\boldsymbol{\delta} I_1$.

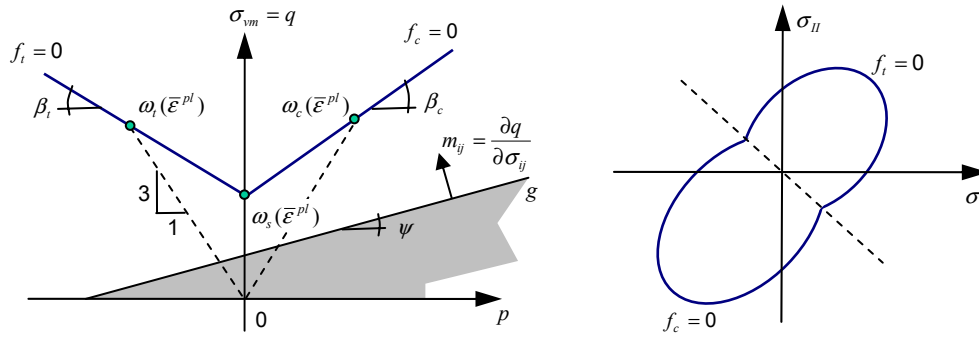


Figure 7: Yield surface and plastic potential in p-q-space and plane stress space

The yield surface in tension f_t , and compression f_c , are defined as:

$$f_t(p, q, \bar{\epsilon}^{pl}) = q - p \tan \beta_t(\bar{\epsilon}^{pl}) - \zeta_s \omega_s(\bar{\epsilon}^{pl}) \quad \text{for } p \leq 0; \quad (3)$$

$$f_c(p, q, \bar{\epsilon}^{pl}) = q - p \tan \beta_c(\bar{\epsilon}^{pl}) - \zeta_s \omega_s(\bar{\epsilon}^{pl}) \quad \text{for } p > 0. \quad (4)$$

Here β_t and β_c are calculated from ω_t , ω_c and ω_s that are gained from direct tension, compression and shear tests, respectively (Figure 8). Note that the elastic component of the strain has to be extracted. Since these modified curves are directly used as input for the material model, β_t and β_c are calculated from

$$\beta_t(\bar{\epsilon}^{pl}) = -3 \frac{\omega_t(\bar{\epsilon}^{pl}) - \omega_s(\bar{\epsilon}^{pl})}{\omega_t(\bar{\epsilon}^{pl})} \zeta_t(\dot{\bar{\epsilon}}^{pl}) \quad \text{and} \quad (5)$$

$$\beta_c(\bar{\epsilon}^{pl}) = 3 \frac{\omega_c(\bar{\epsilon}^{pl}) - \omega_s(\bar{\epsilon}^{pl})}{\omega_c(\bar{\epsilon}^{pl})} \zeta_c(\dot{\bar{\epsilon}}^{pl}). \quad (6)$$

Here $\zeta_t(\dot{\bar{\epsilon}}^{pl})$ and $\zeta_c(\dot{\bar{\epsilon}}^{pl})$ are factors that take strain rate effects in tension and compression into account. It is clear, however, that in cases when rate effects are present, the shear evolution has to be modified also: $\omega_s(\bar{\epsilon}^{pl}, \dot{\bar{\epsilon}}^{pl}) = \omega_s(\bar{\epsilon}^{pl}) \zeta_s(\dot{\bar{\epsilon}}^{pl})$. ζ_t , ζ_c and ζ_s are typically given as tabulated data of strain rate factor vs. strain rate in the input.

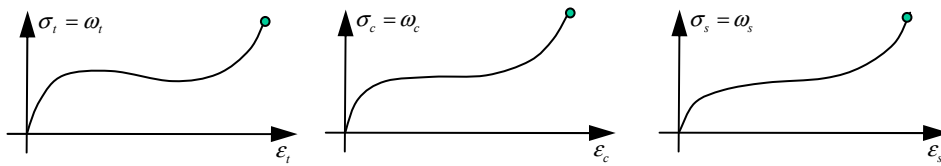


Figure 8: Results from direct tension, compression and shear tests.

The strain rate is obtained by application of a simple filter:

$$\dot{\bar{\epsilon}}^{pl} \Big|_{t+\Delta t} \cong \frac{\Delta \bar{\epsilon}^{pl}}{\Delta t} \Big|_{t+\Delta t} = w \frac{\Delta \bar{\epsilon}^{pl}}{\Delta t} \Big|_{t+\Delta t} + (1-w) \frac{\Delta \bar{\epsilon}^{pl}}{\Delta t} \Big|_t. \quad (7)$$

Usually values of $w = 0.05$ lead to acceptable results.

3.3.2 Plastic potential

The plastic potential g is defined as

$$g = q - p \tan \psi . \tag{8}$$

It should be noted, that with $\psi = 0$ and $\omega_t = \omega_c = \omega_s$ the *von Mises* yield surface is included as special case.

3.3.3 Damage behaviour

Damage is modelled only for unloading to account for the degradation of *Young's* modulus due to plastic loading. Here a simple scalar damage approach has been chosen. The elastic parameter E is scaled by the value $\chi(\bar{\epsilon}^{pl}) = [0,1]$ which is determined from tabulated data. In Figure 9, it is shown how the damage curve can be approximated.

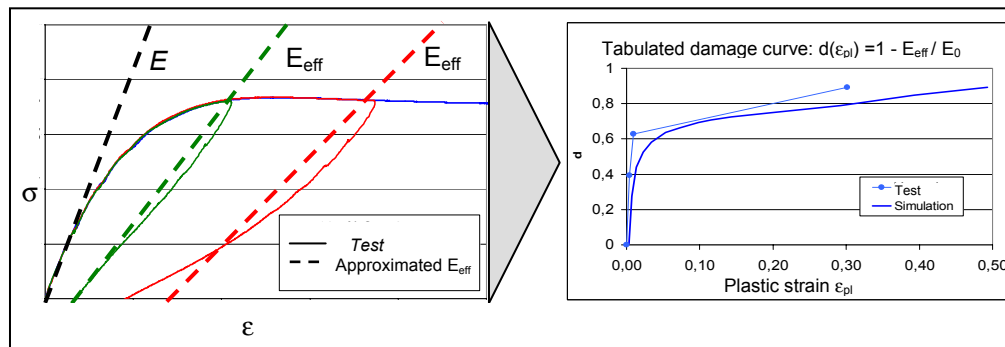


Figure 9: Modelling strategy for a simple damage model

3.3.4 Failure behaviour

Failure, i. e. deletion of elements, is modelled strain rate and pressure dependent. Again tabulated data of two curves is used to define $\bar{\epsilon}_{fail}^{pl} = \bar{\epsilon}_{fail,rate}^{pl} (\bar{\epsilon}^{pl}) \zeta_{fail,pres}(p)$ which determines the onset of element deletion. However, the actual deletion of the element is postponed by a user defined rupture strain $\bar{\epsilon}_{rupt}^{pl}$. In the case of onset of failure the stress in the element is scaled down to

$$\sigma_{fail} = \sigma (1 - \chi_{fade}) \quad \text{where} \quad \chi_{fade} = \left\langle \frac{\bar{\epsilon}^{pl} - \bar{\epsilon}_{fail}^{pl}}{\bar{\epsilon}_{rupt}^{pl}} \right\rangle . \tag{9}$$

Here the *McCauley* notation $\langle \bullet \rangle = \frac{1}{2} (\bullet + |\bullet|)$ is used. The element is finally deleted, if $\chi_{fade} \geq 0.98$ holds true (Figure 10). Thus the effect of fading the failed element smoothly is achieved.

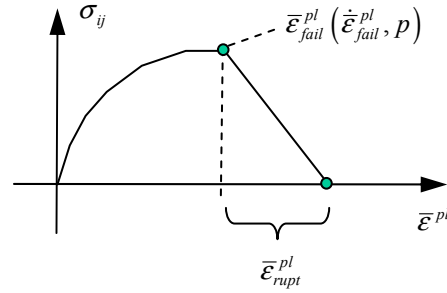


Figure 10: Definition of element failure (fading of element)

3.4 Implementation

The present *SAMP-0* model has been implemented as a user-material in LS-DYNA. Starting from the additive decomposition of the strain increment at time t_{n+1}

$$\Delta \boldsymbol{\varepsilon}_{n+1} = \boldsymbol{\varepsilon}_{n+1} - \boldsymbol{\varepsilon}_n \quad (10)$$

the trial stress, assuming elastic behaviour, is computed as follows:

$$\boldsymbol{\sigma}_{n+1}^{trial} = \boldsymbol{\sigma}_n + \mathbf{C}^{el} : \Delta \boldsymbol{\varepsilon}_{n+1} \quad (11)$$

Checking the yield surface

$$F = F(\boldsymbol{\sigma}_{n+1}^{trial}, \bar{\boldsymbol{\varepsilon}}^{pl}) \quad (12)$$

indicates elastic ($F \leq 0$) or plastic loading ($F > 0$). In the case of plastic loading a classical elastic predictor plastic corrector scheme is applied for stress integration. Here the plastic strain increment can be written as

$$\Delta \boldsymbol{\varepsilon}_{n+1}^{pl} = \boldsymbol{\varepsilon}_{n+1}^{pl} - \boldsymbol{\varepsilon}_n^{pl} = \Delta \lambda_{n+1} \frac{\partial g(\boldsymbol{\sigma}_{n+1})}{\partial \boldsymbol{\sigma}_{n+1}} = \Delta \lambda_{n+1} \mathbf{m}_{n+1}, \quad (13)$$

where g represents the plastic potential, \mathbf{m} the direction of the plastic flow and $\Delta \lambda$ the sought plastic multiplier. The increment of the equivalent plastic strain is obtained from

$$\Delta \bar{\boldsymbol{\varepsilon}}_{n+1}^{pl} = \Delta \lambda_{n+1} \left\| \frac{\partial g(\boldsymbol{\sigma}_{n+1})}{\partial \boldsymbol{\sigma}_{n+1}} \right\| = \Delta \lambda_{n+1} \|\mathbf{m}_{n+1}\|. \quad (14)$$

Hence, the stresses can be calculated through

$$\boldsymbol{\sigma}_{n+1} = \boldsymbol{\sigma}_{n+1}^{trial} - \Delta \lambda \mathbf{C}^{el} : \mathbf{m}_{n+1} \quad (15)$$

and the internal variable is updated by

$$\boldsymbol{\varepsilon}_{n+1}^{pl} = \boldsymbol{\varepsilon}_n^{pl} + \Delta \lambda_{n+1} \|\mathbf{m}_{n+1}\|. \quad (16)$$

Inserting eqn (14) into eqn. (11), where the active yield surface (see eqns. (3) and (4)) is chosen according to the initial trial stress $\boldsymbol{\sigma}_{n+1}^{trial}$ leads formally to

$$F(\boldsymbol{\sigma}_{n+1}, \bar{\boldsymbol{\varepsilon}}_{n+1}^{pl}) = F(\Delta \lambda_{n+1}) = 0. \quad (17)$$

This nonlinear equation in $\Delta\lambda$ is subsequently solved by the standard *Newton-Raphson* method:

$$\Delta\lambda_{n+1}^{j+1} = \Delta\lambda_{n+1}^j - F_{n+1}^j \left(\frac{dF_{n+1}^j}{d\Delta\lambda} \right)^{-1} \quad (18)$$

3.5 Experimental data of yield surfaces of some thermoplastics

In Figure 11 to Figure 13 the yield surface of two different Polycarbonates (PCs) and an ABS [6] are shown and compared to data gained from the fitted standard *Drucker-Prager*-, the *SAMP-0* and the *von Mises* yield loci. While in general the pressure independent *von Mises* yield function is not able to fit the experimental data correctly, both the *Drucker-Prager* and the *SAMP-0* function are in good agreement. However, under biaxial loading some deficiencies for ABS should be mentioned (Figure 13). Also, the standard *Drucker-Prager* model lacks some flexibility when different yield curves for tension and compression shall be taken into account. This could be fixed by a pressure-dependency of the evolution law. But plastic flow will always be towards the same direction (tension for PC and compression for ABS). This has to be considered in a future extension to the *SAMP* model.

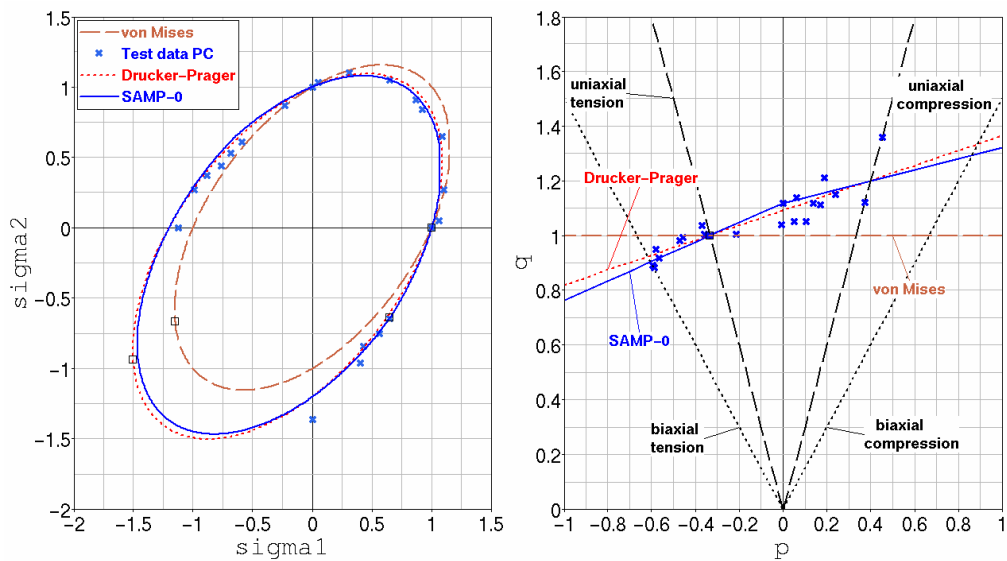


Figure 11: Yield surface of a polycarbonate (PC) -1-

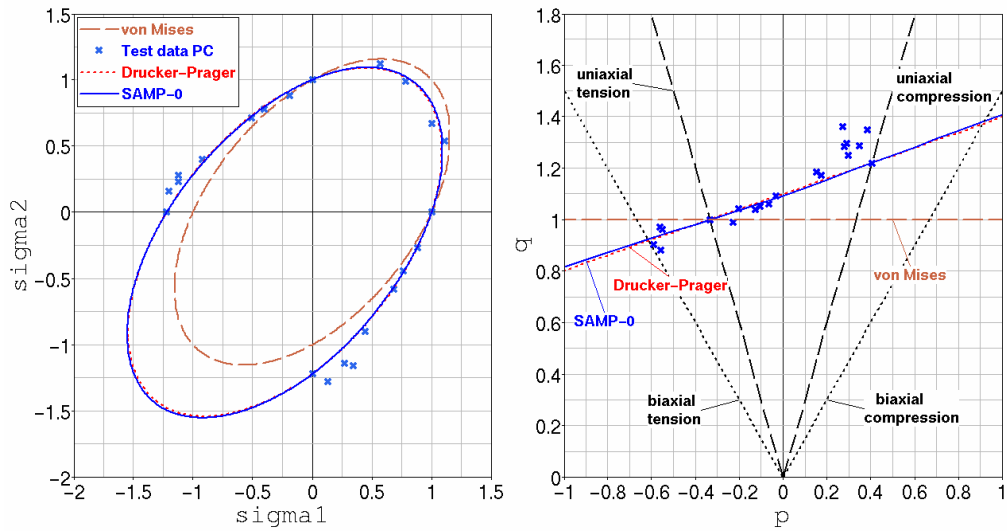


Figure 12: Yield surface of a PC -2-

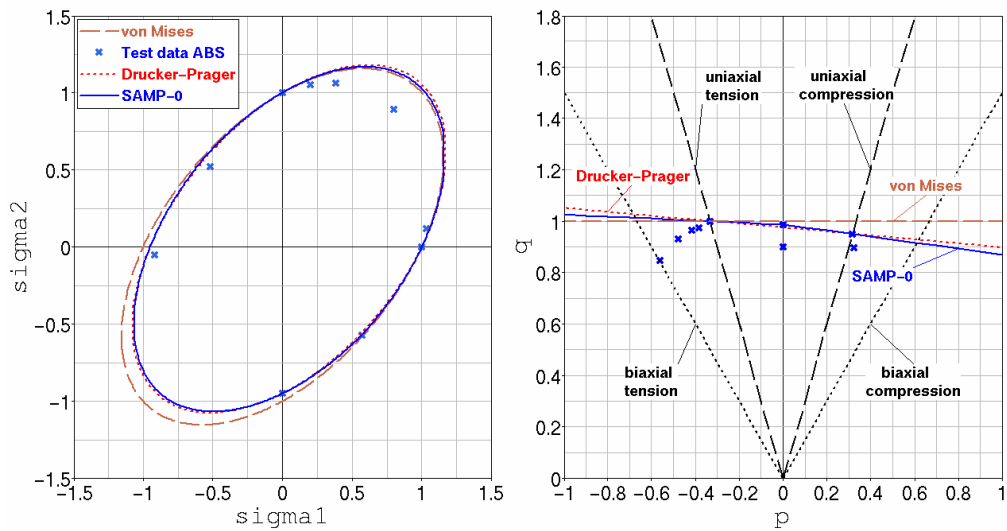


Figure 13: Yield surface of an ABS

3.6 A small numerical test example

In the following a first numerical example of *SAMP-0* is given. Single solid and shell elements that are subjected to tension, compression and shear loading are used to check the implemented algorithm in comparison to a *von Mises* material (for setup see Figure 14). In order to visualize the achieved behaviour the stress-strain-paths are given in Figure 15. It should be mentioned though, that the data was just chosen for numerical testing purposes and do not reflect properties of polymers.

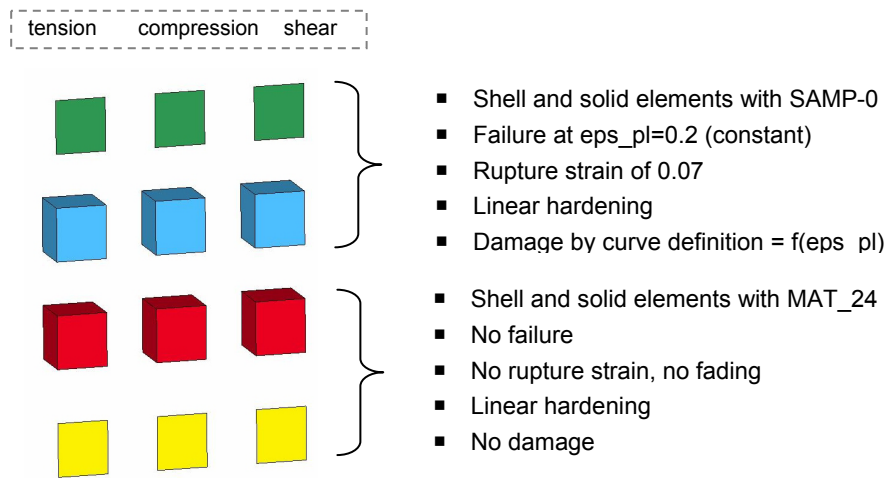


Figure 14: Setup of single element test

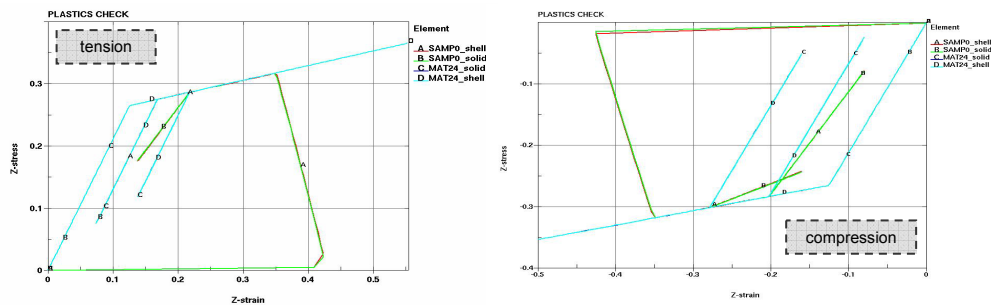


Figure 15: Results of simple tension and compression test for SAMP-0 and MAT_24

4 Conclusions

Thermoplastics are currently modelled in crash simulation using material laws based on *von Mises* plasticity. This approach leaves a lot to be desired. In particular, it is well known that the yield of thermoplastics in tension, compression and shear will not fit a *von Mises* type yield surface. In this paper, we suggest a modelling technique for thermoplastic materials using a modified *Drucker-Prager* yield surface. With this approach, the bending stiffness of the material can be predicted properly which is important for applications in pedestrian or passenger protection. The unloading behaviour is approximated by a simple elastic damage model which represents an important improvement concerning problems where the elastic rebound plays a dominant role, i.e. leg impact in pedestrian protection.

As for future work, the anisotropic hardening of the material due to reorientation of polymer chains has to be taken into account. Furthermore, the consideration of viscosity in the rather “elastic” regime is additionally desirable. Also, the C^0 -continuity condition of the yield surface between f_t and f_c is unsatisfactory and has to be modified as well as the constant dilatancy due to the conical flow rule. Moreover proper failure prediction (damage and crack propagation) for any stress path, as well as consideration of fibre reinforcements are other aspects that need to be addressed in future.

5 References:

- [1] J.O. Hallquist: LS-DYNA, Theoretical Manual, Livermore Software Technology Corporation, Report 1018, 1991.
- [2] P.A. Du Bois: Crashworthiness Engineering Course Notes, Livermore Software Technology Corporation, 2004.
- [3] S. Kolling & A. Haufe: A constitutive model for thermoplastic materials subjected to high strain rates, Proceedings in Applied Mathematics and Mechanics · PAMM, submitted.
- [4] P.A. Du Bois, W. Fassnacht & S. Kolling: General aspects of material models in LS-DYNA. LS-DYNA Forum, Bad Mergentheim, Germany 2002, V2:1-55.
- [5] T. Frank, A. Kurz, M. Pitzer & M. Söllner: Development and validation of numerical pedestrian impactor models. 4th European LS-DYNA Users Conference, pp. C-II-01/18, 2003.
- [6] R. Bardenheier: Mechanisches Versagen von Polymerwerkstoffen. Hanser-Verlag, 1982.
- [7] D.C. Drucker, W. Prager: Soil mechanics and plastic analysis or limit design. Quarterly of Applied Mathematics, 10:157-165, 1952.
- [8] D.C. Drucker: A definition of stable inelastic material. Journal of Applied Mechanics, 26:101-106, 1959.
- [9] P.A. Du Bois, S. Kolling, M. Koesters & T. Frank: Material modeling of polymeric materials in crashworthiness analysis. 3rd Workshop for Material and Structural Behaviour at Crash Processes (*crashMAT*), Freiburg, Germany 2004.
- [10] P. A. Du Bois, S. Kolling, M. Koesters & T. Frank: Material behaviour of polymers under impact loading. International journal of impact mechanics, 2005, in press.
- [11] P.A. Du Bois, M. Koesters, T. Frank & S. Kolling: Crashworthiness analysis of structures made from polymers. 3rd LS-DYNA Forum, Bamberg, Germany 2004. Conference Proceedings, ISBN 3-9809901-0-9, pp. C-I-01/12.
- [12] M. Junginger: Charakterisierung und Modellierung unverstärkter thermoplastischer Kunststoffe zur numerischen Simulation von Crashvorgängen", Dissertation, Fraunhofer Gesellschaft, Germany, ISBN 3-8167-6339-1.

